

# PCCP

Accepted Manuscript



This is an *Accepted Manuscript*, which has been through the Royal Society of Chemistry peer review process and has been accepted for publication.

*Accepted Manuscripts* are published online shortly after acceptance, before technical editing, formatting and proof reading. Using this free service, authors can make their results available to the community, in citable form, before we publish the edited article. We will replace this *Accepted Manuscript* with the edited and formatted *Advance Article* as soon as it is available.

You can find more information about *Accepted Manuscripts* in the [Information for Authors](#).

Please note that technical editing may introduce minor changes to the text and/or graphics, which may alter content. The journal's standard [Terms & Conditions](#) and the [Ethical guidelines](#) still apply. In no event shall the Royal Society of Chemistry be held responsible for any errors or omissions in this *Accepted Manuscript* or any consequences arising from the use of any information it contains.

**Effect of myoglobin crowding on the dynamics of water: an infrared study**

*S. Le Caër,<sup>1\*</sup> G. Klein,<sup>1</sup> D. Ortiz,<sup>1</sup> M. Lima,<sup>2</sup> S. Devineau,<sup>1</sup> S. Pin,<sup>1</sup> J.-B. Brubach,<sup>3</sup> P. Roy,<sup>3</sup> S. Pommeret,<sup>1</sup>  
W. Leibl,<sup>4</sup> R. Righini,<sup>2</sup> J. P. Renault<sup>1</sup>*

<sup>1</sup>*Institut Rayonnement Matière de Saclay*

*LIDyL et Service Interdisciplinaire sur les Systèmes Moléculaires et les Matériaux, UMR 3299  
CNRS/CEA*

*Groupe Physico-Chimie sous Rayonnement, Bâtiment 546*

*F-91191 Gif-sur-Yvette Cedex, France*

<sup>2</sup>*University of Florence, Polo Scientifico,*

*Via Nello Carrara 1,*

*I-50019 Sesto Fiorentino, Italy*

<sup>3</sup>*SOLEIL, CNRS*

*L'Orme des Merisiers, St-Aubin BP 48*

*F-91192 Gif-sur-Yvette Cedex, France*

<sup>4</sup>*CEA*

*SB2SM, iBiTec S, UMR 8221,*

*F-91191 Gif Sur Yvette, France*

**Abstract**

Solutions containing 8 and 32 wt% myoglobin are studied by means of infrared spectroscopy, as a function of temperature (290 K and lower temperatures), in the mid- and far-infrared spectral range. Moreover, ultrafast time-resolved infrared measurements are performed at ambient temperature in the O-D stretching region. The results evidence that the vibrational properties of water remain the same in these myoglobin solutions (anharmonicity, vibrational relaxation lifetime...) and in neat water. However, the collective properties of the water molecules are significantly affected by the presence of the protein: the orientational time increases, the solid-liquid transition is affected in the most concentrated solution and the dynamical transition of the protein is observed, from the point

of view of water, even in the least concentrated solution, proving that the water and myoglobin dynamics are coupled.

## Introduction

Much work has been devoted to the understanding of the dynamics of proteins and to establish links between molecular movements and biological response. Thus, a tight connection was demonstrated between the protein dynamics and the behavior of its solvating water molecules. Indeed, in temperature dependant protein function studies, the onset of protein activities<sup>1</sup> is connected to the solvent dynamics<sup>2-3</sup> through the so called dynamical transition.<sup>4-7</sup>

However, if protein's properties have been shown to depend on water, little attention has been paid to the modifications of water properties<sup>8</sup> in a concentrated protein solution. This point is especially relevant for biological solutions containing a significant weight fraction of macromolecules, in the context of macromolecular crowding.<sup>9</sup>

The purpose of the present study is then to analyze the influence of the well-known globular protein, myoglobin (Mb) on the water structure dynamics through its vibrational properties. To achieve this goal, infrared spectroscopy is used to probe water in concentrated myoglobin aqueous solutions (5 and 20 mmol.dm<sup>-3</sup>): in the mid-infrared, the OH stretching mode is investigated in the 180-300 K temperature range. Again in the mid-infrared region, ultrafast infrared measurements enable to measure vibrational lifetimes and orientational dynamics. Lastly,<sup>10</sup> measurements in the THz region allows to follow changes in water's hydrogen bond network in solute-solution mixtures. THz spectroscopy probes the solvent dynamics on the sub-ps time scale and can measure the extent to which the solute perturbs water. Therefore we performed measurements in the far infrared spectral region (50-350 cm<sup>-1</sup>) in the 100-300 K temperature range, aiming at understanding how the dynamics of water can be affected by the presence of myoglobin.

## Materials and methods

### *Preparation of myoglobin solutions*

Equine heart lyophilized myoglobin was purchased from Sigma (M1882). 1g of myoglobin powder was dissolved in 20 mL of pure water (Elix - Milli-Q system, Millipore, 18.2 MΩ.cm) or of deuterium oxide (D<sub>2</sub>O, 99.90%, Euriso-top). The solutions were respectively dialyzed during 48h at 4°C in 1 L of

H<sub>2</sub>O or 300 mL of D<sub>2</sub>O by changing 3 times the dialysis water (H<sub>2</sub>O or D<sub>2</sub>O). After centrifugation (30000 g, 10 min, 4°C), the myoglobin solution in H<sub>2</sub>O or D<sub>2</sub>O was concentrated to obtain 5 or 18-20 mmol.dm<sup>-3</sup> by passing on centrifugal filter devices Centricon 10 (Amicon Bioseparations, Millipore). The myoglobin concentration was measured from the absorption spectrum recorded on a Shimadzu UV-2450 spectrophotometer ( $\epsilon_{623\text{nm}} = 3500 \text{ dm}^3 \cdot \text{mol}^{-1} \cdot \text{cm}^{-1}$ ).<sup>11</sup> Prior to the experiment, the myoglobin samples were centrifuged (50000 g, 5 min, 4°C) and infrared measurements were performed on the supernatant. The pH of the different solutions is about 7.2.

The density of myoglobin solutions could not be measured because of the limited volumes available but it can be estimated as follows. The partial specific volume of myoglobin in water is known to be 0.741 mL/g.<sup>12</sup> The volumetric mass density of the 5 mmol.dm<sup>-3</sup> (resp. 20 mmol.dm<sup>-3</sup>) solution is then 1.02 g/cm<sup>3</sup> (resp. 1.09 g/cm<sup>3</sup>). The protein weight fraction in the two solutions is respectively 8% and 32%.

#### *Temperature resolved Infrared (FT-IR) spectra*

FT-IR spectra were recorded on a Bruker Vertex 80V spectrometer using the OPUS 6 software. The spectrometer was equipped with a MCT PV detector (Kolmar Technologies), a KBr beam splitter and a temperature-controlled N<sub>2</sub> cryostat (Oxford instruments). The sample holder was equipped with a thermocouple connected to a digital thermometer (Fluke 54 II B). FT-IR spectra were recorded in the 4000-1200 cm<sup>-1</sup> range with a resolution of 4 cm<sup>-1</sup> in the double-sided, forward-backward mode.

Sample films were prepared on CaF<sub>2</sub> windows using aliquots of both myoglobin solutions and a 6 μm thick Mylar spacer. A second CaF<sub>2</sub> window was placed onto the one carrying the solution and sealed with vacuum grease.

#### *Far-Infrared Spectroscopy*

Measurements were performed at the AILES beamline<sup>13</sup> with a Bruker IFS 125 FT-IR spectrometer using the synchrotron far infrared radiation emitted at SOLEIL facility.<sup>14</sup> Spectra from 20 cm<sup>-1</sup> to 700 cm<sup>-1</sup> were obtained by averaging 200 scans with a resolution of 2 cm<sup>-1</sup>, at a 4 cm/s mirror speed. Spectra were recorded using a 6 μm thick Mylar spacer with polyethylene windows, and a 4.2 K bolometer detector with a 20-700 cm<sup>-1</sup> cold filter. Spectra were recorded from 100 to 300 K while the temperature increased by steps of 0.1 K.

#### *Femtosecond infrared pump-probe experiments*

The spectrometer used to measure IR pump-probe spectra is based on a Ti:Sapphire oscillator and regenerative amplifier laser system (Coherent) producing a 1 kHz train of 60 fs, 600 μJ pulses at 800

nm. The output is divided equally to pump two optical parametric amplifiers (TOPAS, Light Conversion Ltd., Vilnius, Lithuania and a home-built OPA) in order to have independently tunable IR-pump and IR-probe pulses. Both pump and probe pulses can be tuned from 3 to 7  $\mu\text{m}$  with a spectral width of about  $250\text{ cm}^{-1}$ . The pump beam passes through a computer controlled delay line and is sent onto the sample together with the probe beam: pump and probe are spatially recombined onto the sample, while the reference crosses a sample zone free from the pump excitation. After their passage through the sample, the probe and the reference are spectrally dispersed into a spectrometer (TRIAX 180, HORIBA Jobin Yvon, Milano, Italy) and detected with an IR array detector.

Finally, a  $\lambda/2$  waveplate is inserted on the pump optical path, in order to change the pump polarization by  $90^\circ$ . The pump pulse is then chopped at a frequency that is half of the repetition rate of the laser (500 Hz) to eliminate the long-term drift of the transient absorption signal. The signal is

defined as: 
$$\Delta A = \log \left( \frac{I_{probe}^{ON} I_{ref}^{OFF}}{I_{probe}^{OFF} I_{ref}^{ON}} \right)$$

where  $I_{probe}^{ON}$ ,  $I_{ref}^{ON}$ ,  $I_{probe}^{OFF}$  and  $I_{ref}^{OFF}$  are respectively the probe and reference signal intensities in the presence and absence of the pump pulse.

The difference absorption signal shows two contributions. One corresponds to the frequency of ground state absorption and arises from the concurrent effect of both the "bleach" (a reduction of the absorption) due to loss of ground state population and the stimulated emission from the first excited state. The other contribution occurs at lower frequency and comes from the  $v = 1 \rightarrow v = 2$  absorption of the first excited state.

In a broadband pump experiment, both pump and probe pulses are spectrally centered roughly on the maximum of the absorption band of the sample. Usually, the pump bandwidth is larger than the absorption bandwidth. Thus all the frequency components of the absorbing system are excited essentially with the same light intensity of the pump. The signal is recorded for two different pump-probe polarizations: parallel ( $\Delta A_{//}$ ) and perpendicular ( $\Delta A_{\perp}$ ). The temporal decay is then evaluated at the magic angle. In this way we isolate vibrational relaxation from rotational effects. Moreover, the decay signal is simulated after 300 fs, in order to eliminate the pump-probe coherent effects. The magic angle signal is fitted and the population relaxation time and the ground state recovery time are calculated.

To obtain information on the rotational dynamics of the water molecules, the anisotropy  $r(t)$  is calculated as: 
$$r(t) = \frac{\Delta A_{\parallel}(t) - \Delta A_{\perp}(t)}{\Delta A_{\parallel}(t) + 2\Delta A_{\perp}(t)}$$
.

More information concerning the fitting procedure and the calculation of the anisotropy (removing the thermal contribution...) can be found in References <sup>15-16</sup>.

## Results

### *Temperature FT-IR spectra in the O-H stretching region (2800-4000 cm<sup>-1</sup>)*

We have focused here our attention on the O-H stretching region, as the H<sub>2</sub>O bending mode (around 1640 cm<sup>-1</sup>) interferes with the CO amide I stretching vibration (around 1650 cm<sup>-1</sup>) and is therefore difficult to interpret. To decipher the contributions arising from the protein itself and from the solution, the mid-infrared spectrum of the lyophilized myoglobin is reported in Figure 1 in Supporting Information.

The evolution of the infrared spectra of water is presented in Figure 1 as a function of temperature in the 2600-4000 cm<sup>-1</sup> spectral range. The band is broad at ambient temperature and centered at 3400 cm<sup>-1</sup>. This band is usually described as arising from three Gaussian components, one around 3300 cm<sup>-1</sup> assigned to strongly H-bonded water molecules; the second one, around 3600 cm<sup>-1</sup> is attributed to poorly hydrogen-bonded water molecules; and the last (around 3460 cm<sup>-1</sup>) to water molecules having an intermediate behavior.<sup>17-18</sup> As temperature decreases, the band is shifted towards the lower energy of the spectrum and the band narrows. Upon freezing, the O-H stretch is seen in the spectrum as a sharp band that increases in intensity as temperature decreases. At 190 K, the band is centered at 3238 cm<sup>-1</sup>, indicating stronger hydrogen bonds than in the liquid phase, as expected.<sup>17</sup> All these observations are in agreement with the well-known formation of hexagonal ice under these experimental conditions. Nevertheless, infrared spectroscopy is not an appropriate tool to distinguish between cubic and hexagonal ice.<sup>19-20</sup> Therefore, the nature of ice will not be discussed in the text. In the case of ice, the full width at half maximum decreases when temperature decreases (Figure 3b), indicating that the H-bond environment becomes more homogeneous.

The spectrum recorded under the same conditions for the 5 mmol.dm<sup>-3</sup> myoglobin sample is presented in Figure 2a. The maximum of the O-H stretching band at 290 K is located at 3400 cm<sup>-1</sup> and the general trends when temperature changes are the same as in pure water. Nevertheless, slight differences between this sample and the water/ice system are found. The shoulders detected at lower wavenumbers, either in the liquid (around 3280 cm<sup>-1</sup>) or in the solid phase (around 3160 cm<sup>-1</sup>),

are more intense than in water. This contribution can be attributed to the NH stretching vibration (amide A band around  $3290\text{ cm}^{-1}$ ; see also the infrared spectrum of lyophilized myoglobin in Figure 1 in Supporting Information).<sup>21</sup> Moreover, the O-H stretching band is broader in this system than in pure water (Figure 3b), indicating a more heterogeneous environment. In the  $5\text{ mmol.dm}^{-3}$  myoglobin sample, the full width at half maximum remains stable on the 180 K-260 K temperature range (Figure 3b), with a higher value than in water, indicating that the H-bond environment remains more disordered than in bulk water and in ice, in the temperature range of this study.

The spectra obtained for the most concentrated myoglobin sample are clearly different from the previous ones (Figure 2b). At ambient temperature, a significant contribution centered at  $3300\text{ cm}^{-1}$  is present. This feature at  $3300\text{ cm}^{-1}$  is attributed to NH stretching vibrations (see the infrared spectrum of lyophilized myoglobin in Figure 1 of Supporting Information in which this band is clearly depicted)<sup>21</sup>. Moreover, this feature can also imply water molecules with strong intramolecular hydrogen bonds within the protein.<sup>22</sup> Additional structures also appear in the tail of the band between  $2800$  and  $3000\text{ cm}^{-1}$ . They are due to CH vibrations of alkyl groups present in myoglobin. Upon freezing, the O-H band still narrows and the maximum at 180 K is located around  $3250\text{ cm}^{-1}$ , which is a value slightly higher than in ice ( $3238\text{ cm}^{-1}$ ). As for the  $5\text{ mmol.dm}^{-3}$  myoglobin sample, the band is significantly broader than in ice, indicating that the environment is clearly more heterogeneous (Figure 3b). It reveals that for all temperatures that the OH bond region is strongly perturbed by the presence of the protein, which is partly due to the interplay with other vibrational modes, such as N-H stretching ones.

The evolution of the area of the O-H band in the three systems, as a function of the temperature and normalized to the value obtained at 240 K, is displayed in Figure 3c. It shows that upon melting the decrease in area between the solid and the liquid phase becomes less pronounced when the myoglobin content increases. In bulk water, the ratio of the absorption of ice versus water is about 1.6 whereas it is about 1.3 in the  $20\text{ mmol.dm}^{-3}$  myoglobin solution. The detailed understanding of the variation in infrared band intensities is usually difficult, but it is tempting to connect such a difference to a change in the refractive index of protein solutions compared to water. This change is related to band intensities in two ways.<sup>23</sup> First, it can change the electromagnetic energy propagation in the considered medium. Following the well-known equation written below and considering a fixed dipole strength  $\mu_D$ , an increase of the band intensity (expressed here as an integral) can arise from a decrease of the refractive index  $n$ :<sup>23</sup>

$$\mu_D^2 = 9.186 \times 10^{-3} n \int [\varepsilon(\tilde{\nu})/\tilde{\nu}] d\tilde{\nu}$$

However, the differences in refractive index between the different samples are not significant enough to account for the observed variation in the infrared band intensities. Indeed, the refractive index of water in the mid infrared is about 1.3, the one of ice is 1.35 and the variation induced by the protein introduction is expected to be in the 0.001 per percent in weight range.<sup>24-25</sup> Second, a change in the refractive index is also the signature of a change in the dielectric constant that can have a substantial impact on oscillator forces. Indeed *ab initio* molecular dynamics studies suggest that dipole correlations control to a large extent the O-H band intensities in water and ice.<sup>26-27</sup> This change in band area observed in Figure 3c could then be put in line with stronger dipole-dipole interactions due to the lower dielectric constant of protein crowded solutions.<sup>28</sup>

Moreover, in the 20 mmol.dm<sup>-3</sup> solution, a significant contribution of the N-H groups is seen in the 2800-4000 cm<sup>-1</sup> band. This contribution is not expected to change with temperature. Therefore the area change of the band upon freezing is smaller than in pure water. Lastly, the smoother solid-liquid transition observed in the most concentrated sample (Figure 3) can be attributed to the large variety of H bonds at the surface or within the protein (for instance water molecules interacting either with hydrophilic sites, or with hydrophobic ones, implying some strong intramolecular H bonds within the protein etc...) which may lead to a gradual solid-liquid transition. This smoother evolution suggests a disorder-broadened first order transition with the coexistence of water domains with melting temperatures at both lower (as usually observed under confinement) and higher than the usual 0°C.

In order to better understand the dynamics in these different systems, ultrafast IR pump-IR probe experiments were undertaken at room temperature (293 K), firstly in the C=O (amide I band) stretching region and secondly in the O-D stretching region.

### Ultrafast IR experiments in the mid-infrared spectral region

#### *The C=O stretching region*

The broad pump pulse is first centered on the maximum of the C=O band (around 1650 cm<sup>-1</sup>).

The C=O spectral region of two myoglobin samples (5 and 18 mmol.dm<sup>-3</sup> respectively, in D<sub>2</sub>O) was studied (around 1650 cm<sup>-1</sup>). This band is known as the amide I band (Figure 1 in Supporting Information). The amide I band implies mainly the C=O stretching mode with small contributions from CN, CCN and NH motions. Its value is characteristic of the secondary structure of the protein, in this case mainly of alpha helices.<sup>29</sup> The measurements are performed in D<sub>2</sub>O to get further from the H<sub>2</sub>O bending mode (the D<sub>2</sub>O bending mode is located around 1210 cm<sup>-1</sup> while its H<sub>2</sub>O counterpart is centered around 1640 cm<sup>-1</sup>). The time-resolved spectra are displayed in Figure 4. The bleaching is observed around 1655 cm<sup>-1</sup> and the induced absorption around 1625 cm<sup>-1</sup>. The vibrational relaxation



can be extracted and is found to be 1.2-1.3 ps for both myoglobin concentrations. The same vibrational relaxation value was obtained in previous works for both myoglobin and different peptides.<sup>30-31</sup> It has been pointed out that this vibrational relaxation time of 1.2 ps is very fast<sup>30</sup> and may be the result of intramolecular energy redistribution (by exciton transfer) in protein secondary structures. Lastly, this relaxation lifetime does not depend on myoglobin concentration, which suggests that the protein backbone dynamics is not modified by crowding on this time scale.

#### *The O-D stretching mode spectral region*

##### Vibrational relaxation

Diluted HOD in H<sub>2</sub>O (12 wt % HOD in H<sub>2</sub>O) was first used as a reference for the comparison between water and the myoglobin solutions. The transient spectra measured after different time intervals in this case are presented in Figure 5 together with the simulations. The bleaching is observed at 2535 cm<sup>-1</sup> whereas an induced absorption is detected at wavenumbers smaller than 2450 cm<sup>-1</sup> (centered around 2400 cm<sup>-1</sup>). A crude estimate of the anharmonicity leads to a value of 135 cm<sup>-1</sup>, which is the difference between the ( $\nu = 0 \rightarrow \nu = 1$ ) transition and the ( $\nu = 1 \rightarrow \nu = 2$ ) transition. The decay of the vibrational population is found to be  $1.4 \pm 0.1$  ps, which is slightly smaller than the value reported for neat water around 2500 cm<sup>-1</sup> ( $1.7 \pm 0.1$  ps).<sup>32</sup> The difference between the two time constants can be related to the differences in D<sub>2</sub>O concentration. As a matter of fact, the concentration used here allows partly the Förster resonant excitation transfer of the O-D stretch mode, resulting in a decrease in the vibrational relaxation lifetime.<sup>33-34</sup> The vibrational lifetime was also studied for myoglobin solutions in the same HOD/H<sub>2</sub>O mixture at a concentration of 5 and 19 mmol.dm<sup>-3</sup>, respectively (Figure 6). In the three cases, the O-D bands in the static infrared spectra are comparable and show no sign of ND formation (see Figure 2 in Supporting Information), indicating that the backbone N-H bonds are not exchanged under our experimental conditions, on the time scale of the experiment (a few hours) in the myoglobin samples. From Figures 5-6, it is clear that the position of the bleaching is progressively shifted towards smaller wavenumbers with increasing times. This apparent shift can be attributed to the thermal contribution which is a negative signal observed at long delay times (see for example the signal obtained at 3.5 ps after the pump pulse). Let's point out that the presence of a negative thermal contribution is consistent with differential spectra obtained in the liquid phase after heating (Figure 2). Having this in mind, it is then clear that within the error bars and within the fluctuation of the maximum energy of the pump, the initial position of the bleaching and of the induced absorption remains similar in the myoglobin samples as in water, leading to the same value for the anharmonicity of the O-D vibrator (140 cm<sup>-1</sup>) as in pure water. A more detailed analysis of the anharmonicity would require the use of the Lippincott-Schroeder model as described in reference<sup>35</sup>.

Nevertheless, it is not necessary in the present case, as the time-resolved spectra remain the same in the three solutions under study, meaning that anharmonicity is the same in the three cases. In the two myoglobin samples, the vibrational lifetime (1.5-1.6 ps) is also very similar to the one obtained in neat water (1.4 ps), indicating that myoglobin has globally no effect on the vibrational lifetime of the individual O-D vibrator.

#### Dynamics of water molecules

The rotational dynamics of water molecules can be probed through the decay time of the anisotropy (Figure 7). The value obtained in neat water (1.3 ps) is faster than the one reported (2.5 ps)<sup>36</sup> probably due to Förster resonant excitation transfer as explained above. As the same average vibrational relaxation time is measured in the three systems, the Förster resonant excitation transfer is expected to remain the same in water and in the myoglobin solutions. Therefore, the evolution of the anisotropy in the three samples can be confidently compared. The decay time of the anisotropy increases from 1.3 ps obtained for water and the 5 mmol.dm<sup>-3</sup> myoglobin solution to 1.9 ps for the 19 mmol.dm<sup>-3</sup> myoglobin solution. Even though the H bond properties do not seem modified from one sample to another, the rotational dynamics becomes slower when the myoglobin crowding increases. In this latter case, a residual anisotropy is also observed at long delay times, in contrast to the water and 5 mmol.dm<sup>-3</sup> myoglobin solution. This residual anisotropy cannot be attributed to the thermal contribution as it is subtracted in the anisotropy calculation (for more details, see reference<sup>16</sup>) but is characteristic of hindered rotational motions in the most concentrated sample.<sup>37</sup> It is then tempting to assign these hindered rotations to frozen water molecules at the protein surface.<sup>38</sup>

Having investigated the mid-infrared region, the dynamics of water can also be probed in the far infrared region where collective motions are detected. This study is performed as a function of temperature in the 100-300 K temperature range to determine if the protein has an impact on the water dynamics.

#### **Far infrared spectra**

##### *Spectra of ice as a function of temperature*

The spectra of ice at different temperatures are given on Figure 8 in the 50-350 cm<sup>-1</sup> spectral range.

The small band at roughly 70 cm<sup>-1</sup> is due to the polyethylene windows and should not be considered here.

The band of ice is broad and extends from 100 to 300 cm<sup>-1</sup> with some characteristic features. At 100 K, a sharp maximum at 231 cm<sup>-1</sup> is observed together with a minimum at 183 cm<sup>-1</sup> and a broader

second maximum around  $168\text{ cm}^{-1}$ . Several shoulders are also detected, mainly around  $196$ ,  $280$  and  $304\text{ cm}^{-1}$ . All these bands are due to the translational lattice vibrations.<sup>39</sup> It must be kept in mind that ice  $I_h$  is an orientationally disordered solid. Forbidden vibrations can be active as the disorder destroys the hexagonal symmetry. The band around  $230\text{ cm}^{-1}$  is due to transverse optic vibrations while the features above  $300\text{ cm}^{-1}$  are dominated by longitudinal optic vibrations. The shoulder around  $190\text{ cm}^{-1}$  is attributed to longitudinal optic mode and the band around  $160\text{ cm}^{-1}$  to the longitudinal acoustic modes.<sup>19</sup> In other words, the two bands around  $230$  and  $160\text{ cm}^{-1}$  correspond to intermolecular hydrogen bond stretching motions, but with motions having different directions.<sup>40-41</sup> However recent first principle dynamic simulations suggest that the vibrations should rather be described as a collective mode in liquid water.<sup>26, 42</sup>

When temperature increases from  $100$  to  $270\text{ K}$ , the general features of the band remain the same but they shift to lower wavenumbers. The amplitude of the sharp maximum decreases and is shifted to  $214\text{ cm}^{-1}$ . The minimum is now observed at  $168\text{ cm}^{-1}$  and the broader second maximum is less intense and located at  $155\text{ cm}^{-1}$ . One shoulder is still observed at  $278\text{ cm}^{-1}$ .

The evolution of the maximum of the band with temperature is currently interpreted as the signature of the anharmonicity of the hydrogen bond network.<sup>43</sup> As temperature increases, hot bands (i.e. transitions from excited levels) appear at lower wavenumbers and account for the shift and the broadening of the band.<sup>39</sup>

#### *Spectra of myoglobin solutions at 5 and 20 mmol.dm<sup>-3</sup>*

It is well known that the far infrared spectra of proteins in aqueous solutions are completely dominated by the water signal.<sup>44</sup>

The spectra of the myoglobin samples at  $5$  and  $20\text{ mmol.dm}^{-3}$  are displayed in Figure 9. Globally, the main characteristics of the band resemble bulk ice (or bulk water for the liquid phase), for the two myoglobin/water systems. Far infrared spectra (Figures 8-9) help answering to the question whether ice can be amorphous in the crowded samples, as amorphous ice has a markedly different signature from cubic or hexagonal ice.<sup>45</sup> These spectra at low temperature reveal clearly that ice is not amorphous, even in the most concentrated myoglobin system. The comparison between the different spectra obtained in the solid phase is depicted in Figure 10, where the spectra obtained at  $150\text{ K}$  are normalized using the most intense band. The positions of the two maxima and of the minimum remain the same in all three samples in the temperature range retained here (see Figure 3 in Supporting Information for the case of the evolution of the position of the sharp maximum). As the shift of the position of the bands with temperature is linked to the anharmonicity of the system, it

appears here that anharmonicity remains the same in the systems under study. This point is in agreement with the ultrafast infrared experiments.

Nevertheless, some differences between the systems can also be depicted. At 100 K, for the 20 mmol.dm<sup>-3</sup> system, shoulders can be observed at roughly 204, 272 and 306 cm<sup>-1</sup>. The most striking feature here is the enhanced contribution of infrared modes in the 100-325 cm<sup>-1</sup> wavenumber range (see Figure 10) in the case of the most concentrated myoglobin sample. Indeed the ratio of the first to second maximum varies from 3:1 in bulk water and for the 5 mmol.dm<sup>-3</sup> protein sample down to 2:1 in the 20 mmol.dm<sup>-3</sup> myoglobin sample. The feature at wavenumbers greater than 240 cm<sup>-1</sup> was attributed to anharmonicity and/or long range electrostatic effects.<sup>41</sup> As this enhanced contribution cannot be linked to a change in anharmonicity (see above), it is tempting to connect it to a change in electrostatic interactions<sup>46</sup> due to the decrease of the dielectric constant in crowded environment.<sup>28</sup> However, we cannot exclude also that an increase of the ice disorder (as suggested by the O-H stretching band) would also lead to a relaxation of the selection rules.

We would also like to comment on the evolution of the baseline underlying the 50-350 cm<sup>-1</sup> band.

Comparison of Figures 8 and 9 evidences that the baseline becomes more pronounced in the most concentrated sample for temperatures above 200 K. This baseline corresponds in fact to the tail of the libration band (or hindered rotational band). This band was studied by means of quasi elastic neutron scattering measurements in the case of hydrated myoglobin samples.<sup>47</sup> It was proven in this case that the librational band of water in the myoglobin/water system broadens significantly when temperature increases. This broadening can account for the baseline change observed in the 20 mmol.dm<sup>-3</sup> sample when temperature increases (Figure 9).

Another striking difference between the spectra of myoglobin samples and ice one arises from their respective band area evolution as a function of temperature (Figure 11). These changes are reported here after subtracting the baseline from the spectra. This removal of the libration contribution allows focusing only on the translational lattice modes. On this figure, and contrary to the evolution of the band area of ice, for which a decrease is observed on the temperature range studied, an abrupt change at 200 K in the amplitude and in the area of the translational band is depicted for both myoglobin samples. This is indicative of the dynamical transition of myoglobin which is traditionally observed from the mean square displacements of the protein and the heme iron.<sup>47</sup> The transition observed here from the point of view of water occurs then at the same temperature as the protein transition,<sup>48-50</sup> revealing therefore a coupling between the protein dynamics and the solvent dynamics. Lastly, let's point out here that this transition is also observed for the lowest myoglobin concentration.

## Discussion

The O-H stretching region of liquid water is classically used to identify particular behaviors. Indeed, in the case of crowded protein solutions, the spectra recorded in water and in the two myoglobin samples in the O-H spectral region differ significantly, especially between water and the most concentrated myoglobin solution (Figures 1-2). Nevertheless, the infrared signature in this latter case is difficult to interpret in this case because of the presence of NH stretching modes and also of the alkyl groups arising from the protein.

In the following, we show that the use of temperature variations enables to unravel subtle differences, which can be put in line with the water structure in protein solutions.

For one myoglobin molecule, there are roughly 2000 water molecules in the 20 mmol.dm<sup>-3</sup> myoglobin solution, and 10400 water molecules in the 5 mmol.dm<sup>-3</sup> solution. The van der Waals surface of one myoglobin molecule was computed to be about 16200 Å<sup>2</sup>, whereas the solvent accessible surface area is calculated to be about 8300 Å<sup>2</sup>.<sup>51</sup> Knowing the surface area of a water molecule (20 Å<sup>2</sup>)<sup>52</sup>, roughly 400 water molecules have access to the protein surface, which is consistent with a value of 350 water molecules hydrating myoglobin determined by molecular dynamics simulations<sup>38</sup>. This implies that, in the most concentrated solution, 20% of the water molecules interact directly with myoglobin; and a mere 4% of the water molecules interact with the protein in the 5 mmol.dm<sup>-3</sup> solution. As shown by SAXS measurements,<sup>53</sup> the myoglobin solution structure is quite well described by the hard sphere approximation. The radius for equivalent spheres was calculated to be about 20 Å in the case of myoglobin.<sup>53</sup> In SAXS measurements, the solution structure factor gives access to the minimal distance between neighboring proteins. At high concentration (0.3-0.4 g.mL<sup>-1</sup> or around 20 mmol.dm<sup>-3</sup>), this distance is found to be 37 Å which is about 2 protein radii. It means that most water molecules are located in the pores created by the protein packing/jamming. Torquato and coworkers<sup>54</sup> characterized the dimension of such pores for hard sphere liquids, and showed that it depends only on the volume fraction  $\Phi$  and on the hard sphere radius. For a myoglobin concentration of 20 mmol.dm<sup>-3</sup>, the protein volume fraction is 0.26.<sup>12</sup> We must notice that the disappearing of the colloid diffusion (also called the colloidal freezing point) is expected to occur at  $\Phi = 0.5$ . We are well below this limit, which explains why the solution is still macroscopically fluid. The average pore size obtained for  $\Phi = 0.26$  is expected to be about  $0.4 \pm 0.15$  protein radius, i.e. about 8 Å. At 5 mmol.dm<sup>-3</sup> ( $\Phi = 0.06$ ), the average pore size will be roughly  $1.1 \pm 0.3$  protein radius, i.e. about 22 Å. It implies that most water molecules are not adsorbed on the surface of the protein, even in the most concentrated sample but are present as nano-droplets inside nanometric pores between

myoglobin molecules. Therefore, our results can be compared to the ones obtained for other types of confined water, such as water in micelles (soft confinement)<sup>55-56</sup> or in porous glasses (rigid confinement)<sup>18</sup>.

On one hand, in the present study, the vibrational O-D relaxation time does not change when the myoglobin content increases. It is well known that the relaxation process depends on structural factors, such as the O...O distance distribution, the average number of hydrogen bonds etc...<sup>57</sup> Our results prove then that these structural factors are not significantly modified between water and myoglobin solutions. Moreover, the anharmonicity of the O-D vibrator remains the same in all three cases (Figures 5-6), which is also consistent with the measurements performed in the far infrared spectral region. Water molecules remain unchanged; and the differences in the 2800-4000  $\text{cm}^{-1}$  spectral region (Figures 1-2) are due to the interferences of contributions arising from the protein itself. This observation is qualitatively different from both hard<sup>18, 57</sup> and soft confinement<sup>56</sup>, where relaxation times are usually significantly altered by small pore sizes. The question is now whether the surface of the protein is globally more "water-like" than the other types of confining walls.

On the other hand, differences appear for the collective motions of water molecules in crowded solution. The orientational time increases in the most concentrated solution (Figure 7), while the anisotropy remains high, even at long delay times (Figure 7). The increase in the orientational time with the myoglobin content can be attributed to an increase in the (local) solvent viscosity.<sup>58</sup> Moreover, the residual anisotropy at long times (4-5 ps, Figure 7) observed in the most concentrated solution can be linked to the 350-500 water molecules interacting with the protein surface which hinders their rotational motions.<sup>38</sup> A special comment is required here on the significance of the change in water rotational dynamics and on the connection between local (nanoscopic) and macroscopic viscosity.<sup>59</sup> Previous studies on crowded solutions have shown that the viscosity depends strongly on the length scale considered. On length scales larger than the macromolecule size, and up to the macroscopic scale, the viscosity is completely controlled by the macromolecule concentration due to excluded volume effects and mobile obstacles.<sup>60</sup> On a scale smaller than the macromolecule, a minimal effect of the crowding is expected. Therefore, even in crowded solutions, the local viscosity of water is not expected to be modified. The 5  $\text{mmol}\cdot\text{dm}^{-3}$  myoglobin solution is a clear example of this behavior. The reduced viscosity was evaluated to be around 4.9  $\text{mL}\cdot\text{g}^{-1}$  for a myoglobin solution at a 5  $\text{mmol}\cdot\text{dm}^{-3}$  concentration,<sup>58</sup> corresponding to a 50 % increase in the macroscopic viscosity as compared to water, whereas the nanoscopic viscosity measured here by water reorientation is not modified with respect to bulk water (Figure 7). However, this rule is not respected for the highest myoglobin concentration, where the nanoscopic viscosity is increased by the crowding (Figure 7). This effect can be easily understood by considering that, in these solutions

having sub-nanometric pores, a large proportion of the water molecules are in interaction either with the protein or with the surface which results in a significantly perturbed dynamic of these molecules. Such a phenomenon was already observed for water in either rigid or soft confinements: surface water has limited reorientational motions,<sup>57, 61</sup> but it has a preeminent importance in a biological context where all biochemical reactions will depend on this nanoscopic viscosity.

Lastly, measurements performed in the far-infrared energy range give a complementary picture of the influence of the protein on the water bonding. Contrary to what was observed in hard<sup>18</sup> and soft<sup>56</sup> confinement, the room temperature far IR spectrum does not give any indication of a change in the H bond stretching. The spectra recorded as a function of temperature indicate that anharmonicity does not change in protein solutions (Figures 8-10), in agreement with the ultrafast infrared experiments. The increase in the absorbance observed at wavenumbers greater than 240  $\text{cm}^{-1}$  in the 20  $\text{mmol}\cdot\text{dm}^{-3}$  sample (Figure 10) can be attributed to a change in relative band intensities.<sup>26</sup> Moreover, the change in the tail of the librational band observed in the 20  $\text{mmol}\cdot\text{dm}^{-3}$  sample (Figure 9) is also in line with the change in the orientational dynamics evidenced in this case (Figure 7). The change in collective hydrogen bond dynamics observed in the most crowded sample is in line with recent molecular dynamics simulations<sup>62</sup> which have evidenced that correlated protein and water motions extend up to 1 nm from the protein surface. This is in line with the 2.2 nm water pore size diameter (or a 1.1 nm radius) present in the most crowded solution as explained above. Other recent calculations<sup>63</sup> have also evidenced the presence in the water dynamics of collective modes arising from the protein. In 1 nm, there are roughly 4 water layers (the size of one water layer being around 2.5 Å), meaning that in the corresponding volume of a sphere having a radius of 1 nm, there are roughly 250 water molecules. The collective motions concern then a few hundreds of water molecules.

Our result provide a global picture of water in crowded protein environment: contrary to most other confining systems, proteic confinement does not significantly modify the water H bond network. The most obvious confirmation of this fact is that, even in a crowded myoglobin system, water still freezes at 273 K. Nevertheless, despite this preservation of the native water H bond, water dynamics can be deeply affected by the protein confinement, leading to a significant increase of nanoscopic viscosity. This last point confirms, if necessary, that the water dynamics can be, to some extent, decoupled from the H bond properties. In these systems, the collective properties are enhanced, but with no structural counterpart.

We cannot end this paper without a short comment on the impact of protein dynamical transition on water properties, even in the 5  $\text{mmol}\cdot\text{dm}^{-3}$  myoglobin solution (Figure 11). Molecular dynamics

simulations<sup>48</sup> performed on myoglobin with a shell of water molecules have evidenced that this transition is due to the translational hydration water dynamics. When these translational motions begin, increased fluctuations in side chains of the protein appear. This picture is consistent with our observations. However, the common idea is that the solvent dynamics imposes the biomolecule dynamics.<sup>6</sup> Our study proves that even if water drives the protein dynamical transition, the protein itself has an influence on water dynamics. Water is not the « master » and myoglobin is not the « slave »: both species are coupled,<sup>64</sup> the transition leading to a global increase of their dynamics.<sup>65</sup>

### Conclusion

In the present study, we have focused our attention on crowded myoglobin solutions rather than on water molecules interacting with a protein powder. Ultrafast mid-infrared experiments, but also mid- and far-infrared experiments performed at ambient and lower temperatures enable us to conclude that the individual properties of the water molecules, such as anharmonicity and vibrational relaxation time, are not affected by the protein. Nevertheless, the collective properties of water are significantly modified in the crowded solutions. In ice, the features above  $240\text{ cm}^{-1}$  in the far-infrared spectra are thus clearly enhanced in the 32 wt% protein sample, indicating that anisotropic long range electrostatic effects are more intense. The rotational dynamics is also slowed down in this case, which can be linked to a change in the viscosity of the crowded sample. The solid-liquid transition around 273 K is smoother than for water, which is in line with a more heterogeneous H-bond environment. Last but not least, the dynamical transition of the protein is detected in the far infrared spectra of ice, both in the 8 and 32 wt% myoglobin samples. The collective motions which are affected by the presence of myoglobin extend upon a few hundreds of water molecules.

### Acknowledgments

This work was supported by the French Infrastructure for Integrated Structural Biology (FRISBI) ANR-10-INSB-05-01.

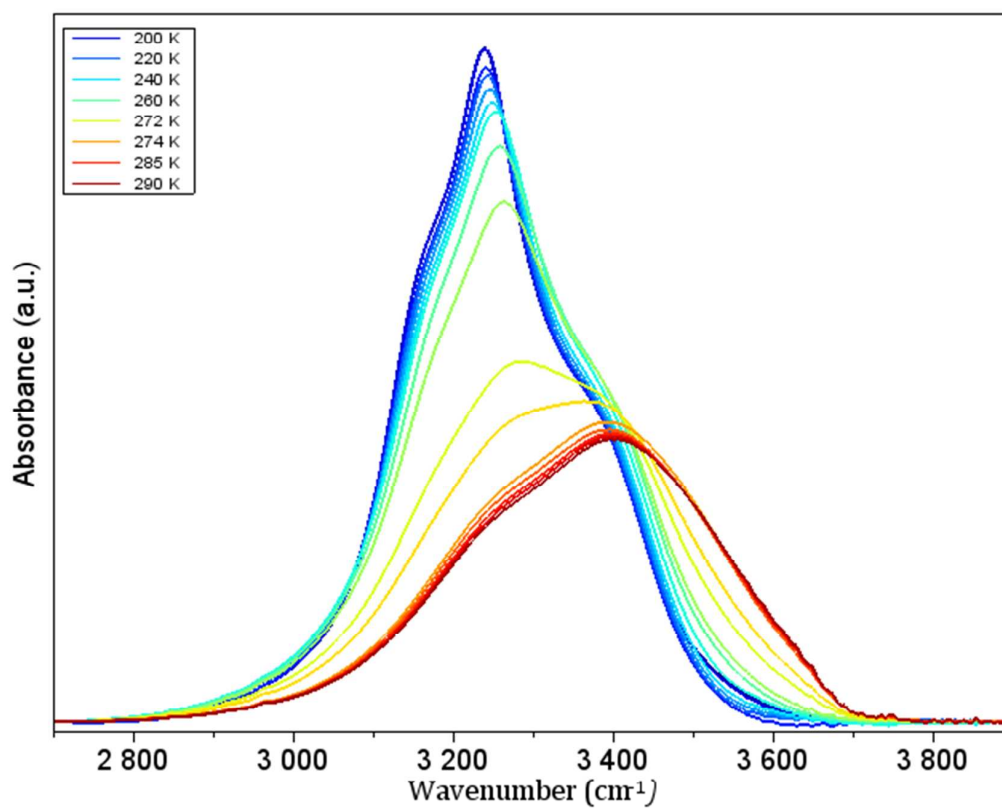
The ultrafast infrared results were obtained thanks to the funding from the European Community's Seventh Framework Program under Grant Agreement No. 228334.

We acknowledge SOLEIL for provision of synchrotron radiation facilities.



## Figures

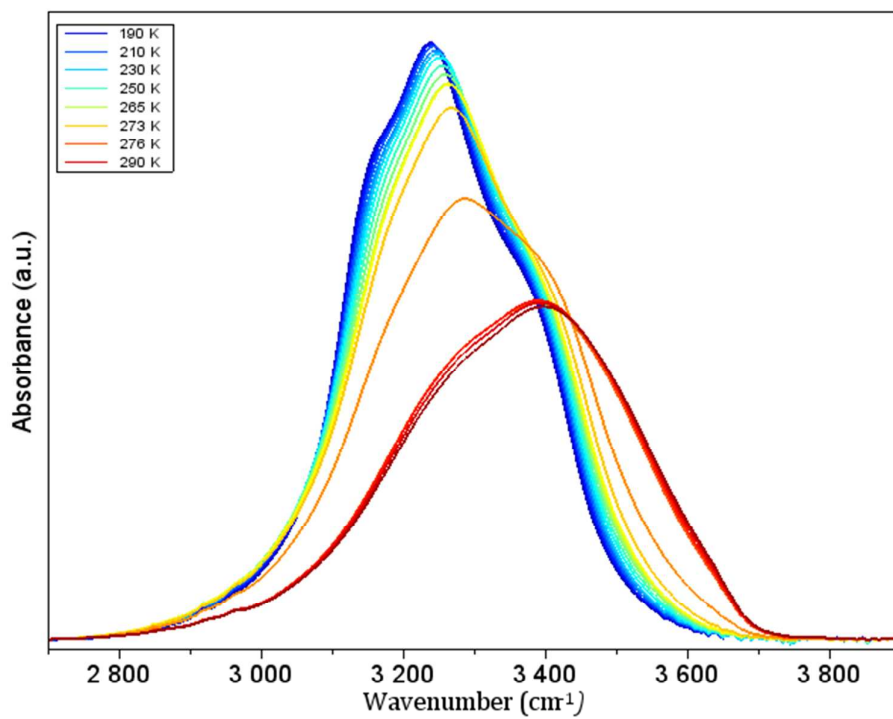
Figure 1



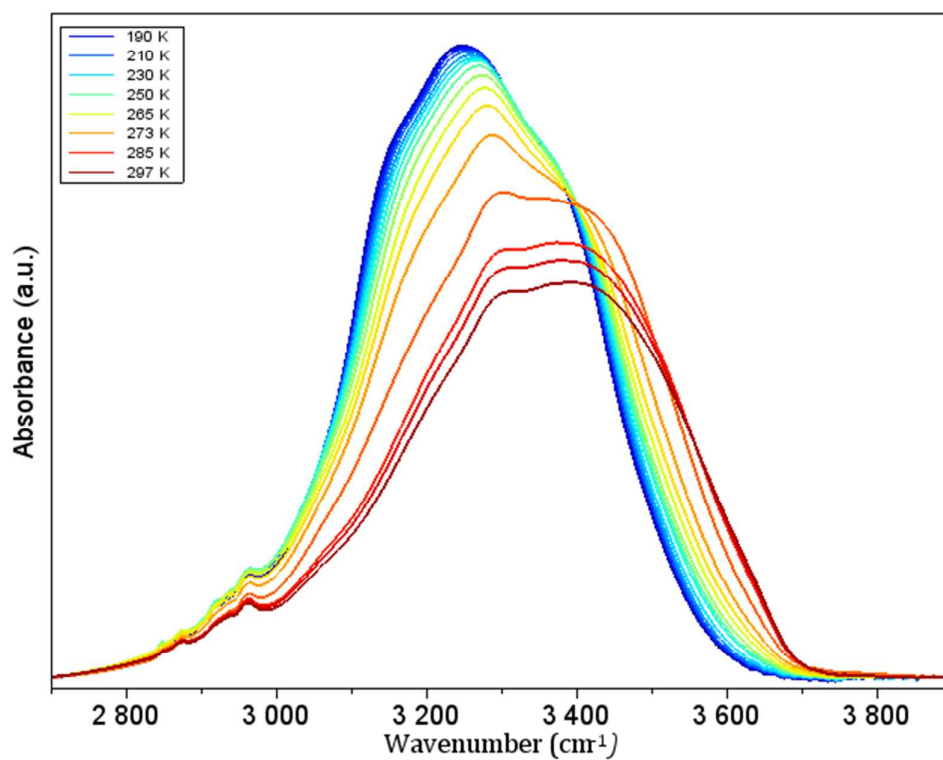
*Spectra of ice and water in the O-H stretching region (2800-4000  $\text{cm}^{-1}$ ). The temperature ranges from 190 K (blue) to 290 K (brown). Spectra are recorded by increasing the temperature by steps of 10 K. More spectra are recorded around the solid-liquid transition (273 K).*

Figure 2

(a)



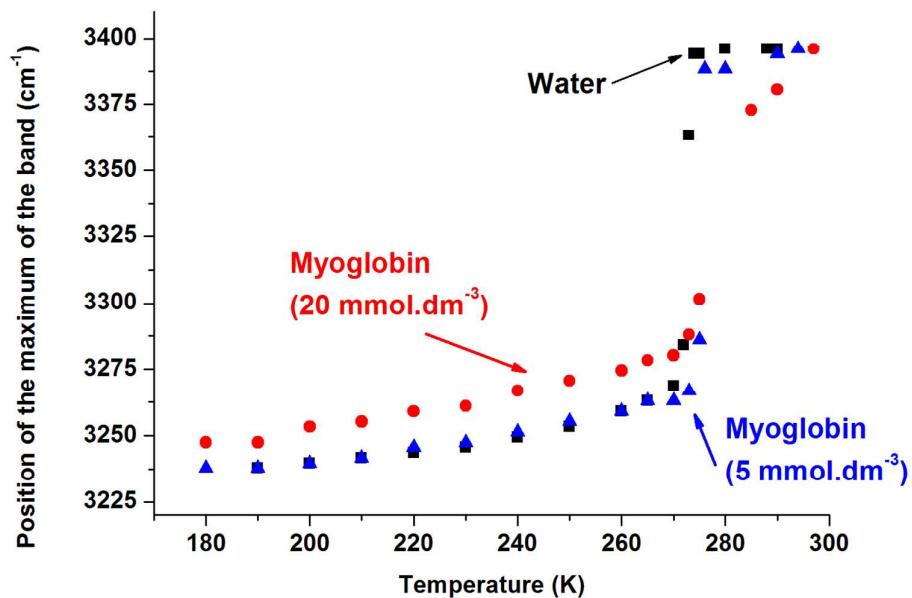
(b)



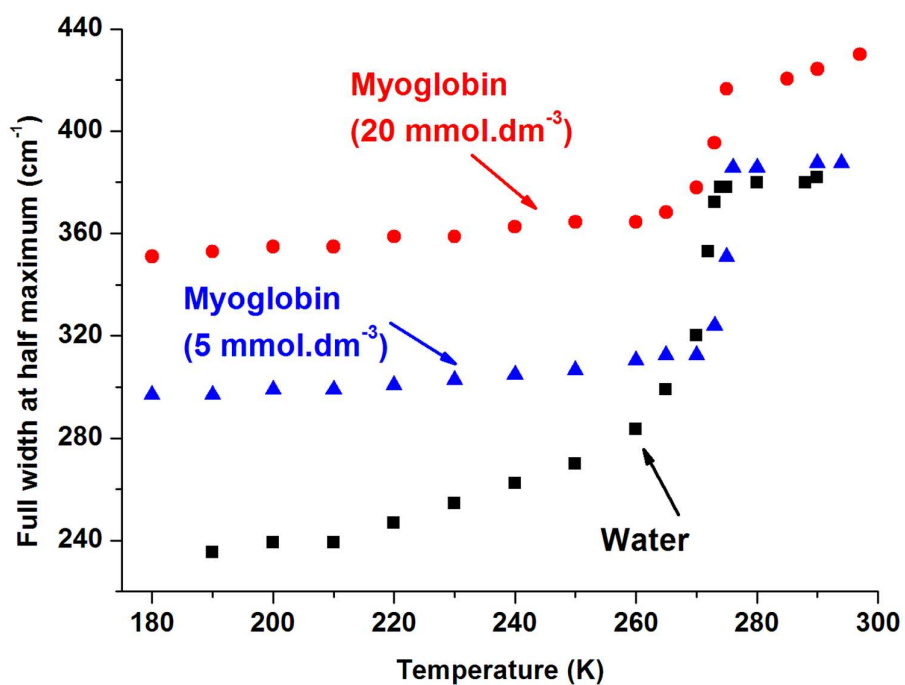
Spectra in the O-H stretching region ( $2800\text{-}4000\text{ cm}^{-1}$ ) obtained from a  $5\text{ mmol}\cdot\text{dm}^{-3}$  myoglobin solution (2a) and a  $20\text{ mmol}\cdot\text{dm}^{-3}$  myoglobin solution (2b). The temperature increases from 180 K (blue) to 294 K (brown) by step of 10 K in Figure 2a; and from 180 K (blue) to 297 K (brown) in Figure 2b. More spectra are recorded around the solid-liquid transition (273 K).

Figure 3.

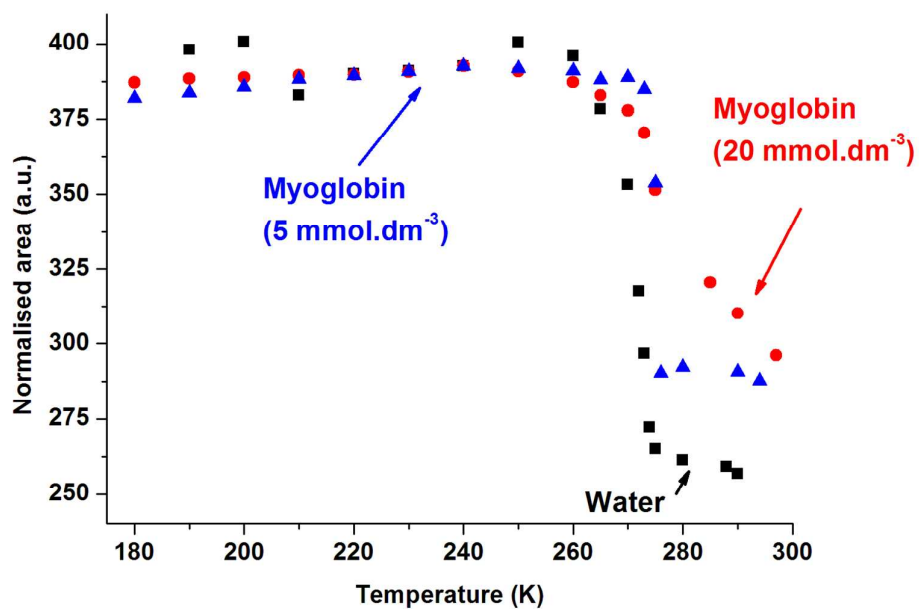
(a)



(b)

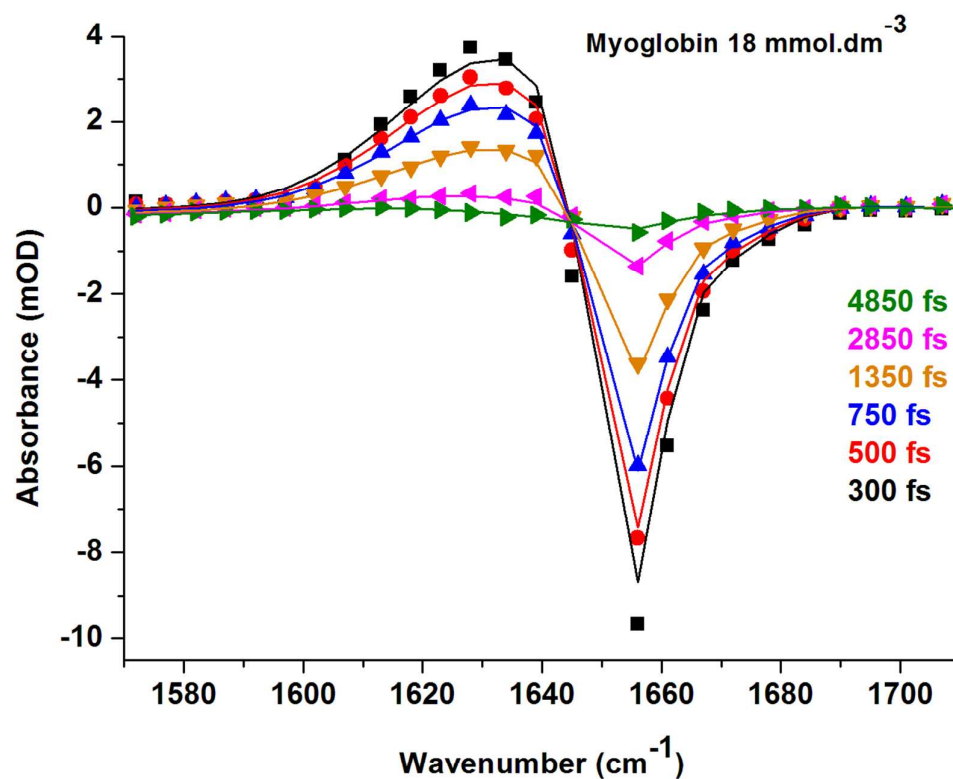


(c)



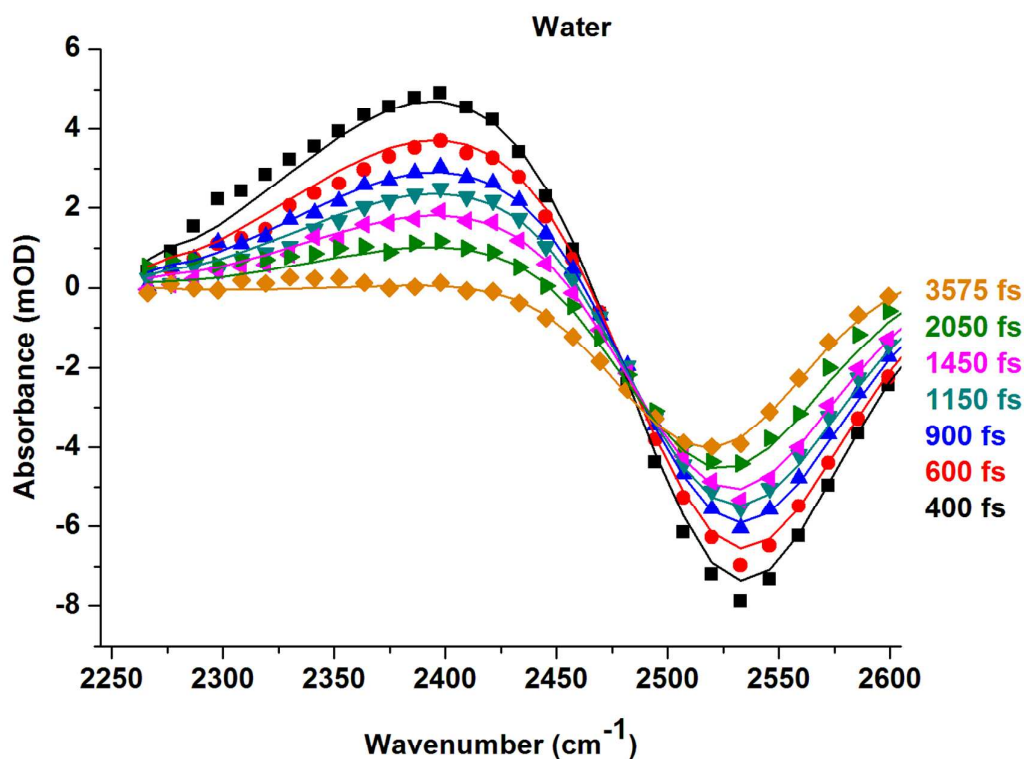
Evolution of the maximum position of the O-H stretching band, of the full width at half maximum of the band and of the area in the  $2600\text{-}4000\text{ cm}^{-1}$  spectral region as a function of the temperature for water (black squares), the  $5\text{ mmol.dm}^{-3}$  myoglobin solution (blue triangles) and the  $20\text{ mmol.dm}^{-3}$  myoglobin solution (red circles). All the areas of the O-H band are normalized to their value at 240 K, which is a temperature region in which the area of the O-H band changes only slightly in the three cases.

Figure 4.



Time-resolved spectra obtained at room temperature (293 K) by broadband femtosecond IR-pump IR-probe spectroscopy in the CO stretching region (amide I band) for the 18 mmol.dm<sup>-3</sup> myoglobin solution in D<sub>2</sub>O. The symbols correspond to the experimental points and the lines to the simulations of the spectra at different delay times after the pump impulsion (■, 300 fs; ●, 500 fs; ▲, 750 fs; ▼, 1350 fs; ◀, 2850 fs and ▶, 4850 fs). The time-resolved spectra obtained for the 5 mmol.dm<sup>-3</sup> myoglobin solution are very similar and are therefore not presented here.

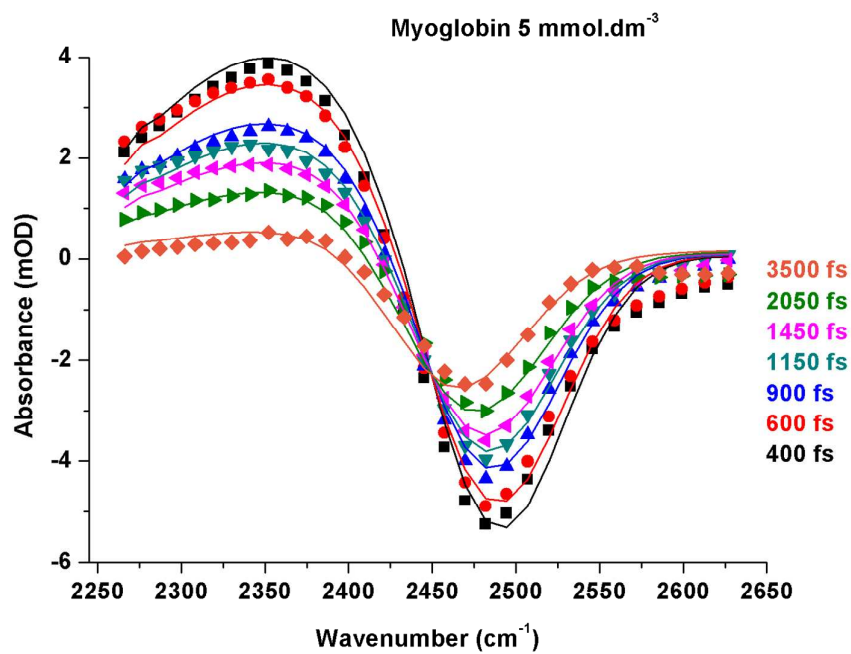
Figure 5.



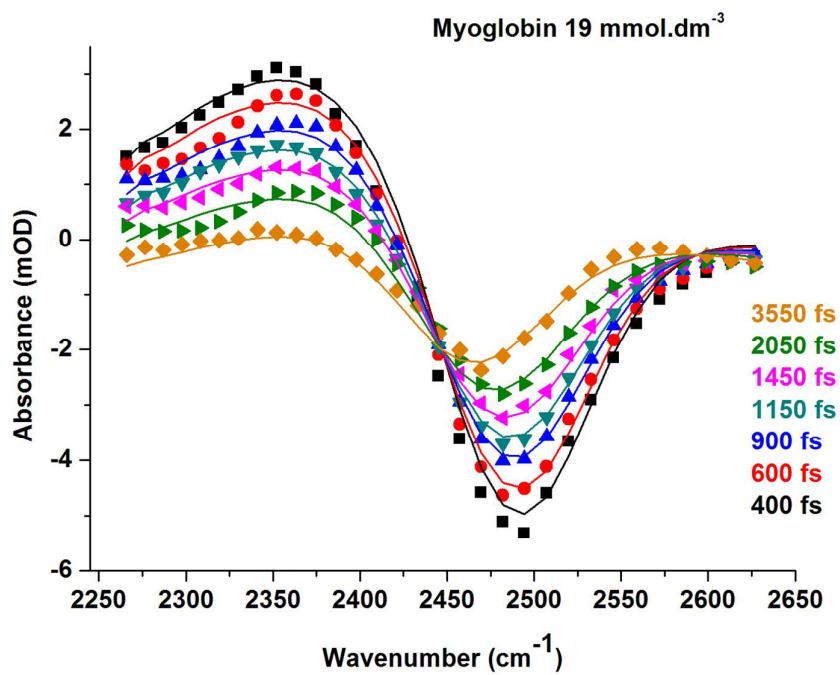
Time-resolved spectra obtained at room temperature (293 K) by broadband femtosecond IR-pump IR-probe spectroscopy in the O-D stretching region of pure water (12% HOD in  $\text{H}_2\text{O}$ ). The symbols correspond to the experimental points and the lines to the simulations. The spectra are given at 400 fs (■); 600 fs (●); 900 fs (▲); 1150 fs (▼); 1450 fs (◄); 2050 fs (►) and 3575 fs (◆) after the pump impulsion.

Figure 6.

(a)



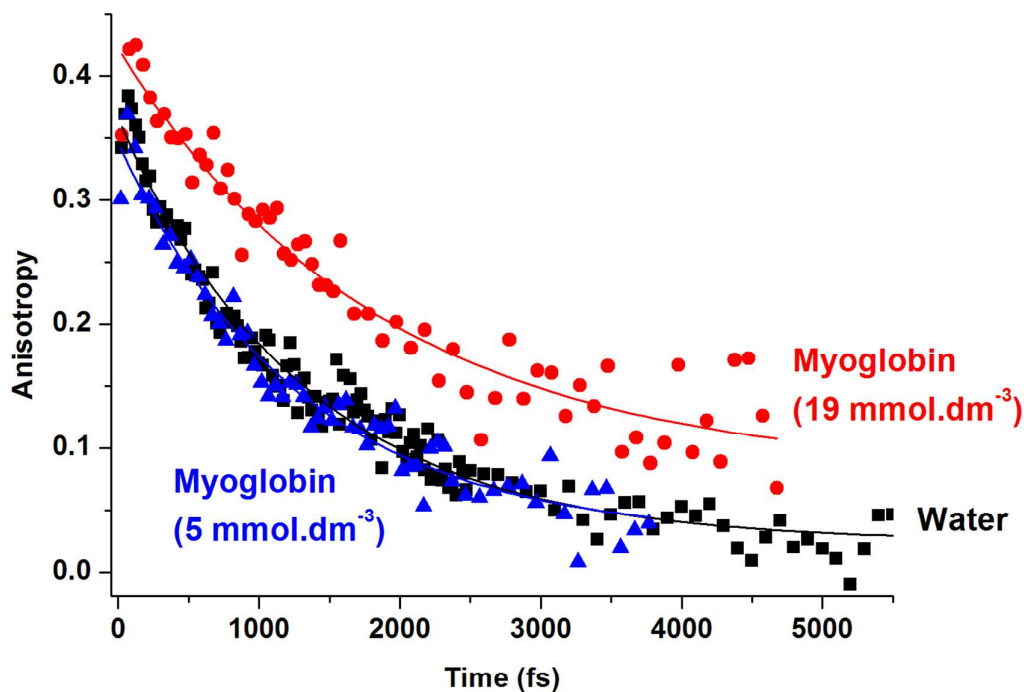
(b)





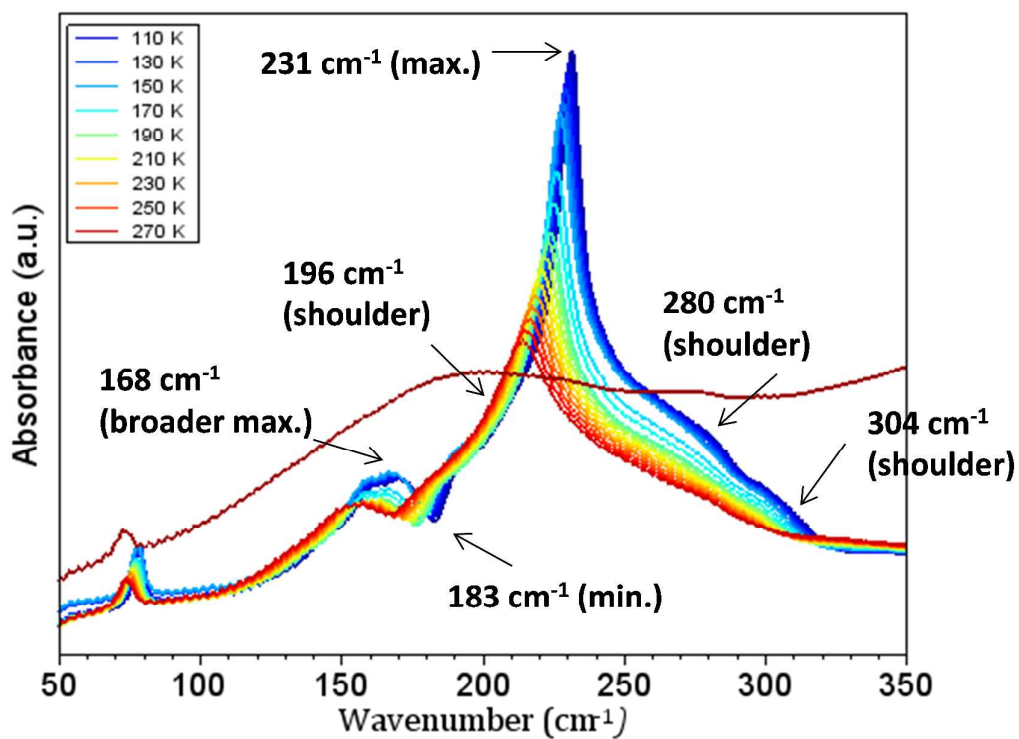
*Time-resolved spectra obtained at room temperature (293 K) by broadband femtosecond IR-pump IR-probe spectroscopy in the OD stretching region of a 5 mmol.dm<sup>-3</sup> (5a) and a 19 mmol.dm<sup>-3</sup> myoglobin solution (in a 12%HOD/H<sub>2</sub>O mixture). The symbols correspond to the experimental points and the lines to the simulations. The spectra are given at 400 fs (■); 600 fs (●); 900 fs (▲); 1150 fs (▼); 1450 fs (◀); 2050 fs (▶) and 3500 fs for 6a and 3550 fs for 6b(◆) after the pump impulsion.*

Figure 7.



Evolution of the anisotropy obtained at room temperature (293 K) for water (black squares), the  $5 \text{ mmol.dm}^{-3}$  myoglobin solution (blue triangles) and the  $19 \text{ mmol.dm}^{-3}$  myoglobin solution (12% HOD/H<sub>2</sub>O mixture) (red circles). The symbols are experimental points and the lines are obtained with decaying exponential functions. The decays of the anisotropy of water and of the  $5 \text{ mmol.dm}^{-3}$  myoglobin solution are fitted with the respective functions:  $0.02+0.34*\exp(-t/1300)$  and  $0.03+0.32*\exp(-t/1300)$ , where  $t$  is expressed in fs. The decay of the  $19 \text{ mmol.dm}^{-3}$  myoglobin solution is well represented by the function  $0.08+0.34*\exp(-t/1900)$ , with  $t$  expressed in fs. In this latter case, anisotropy remains at high values even at long delay times, indicating that rotational motions are hindered.

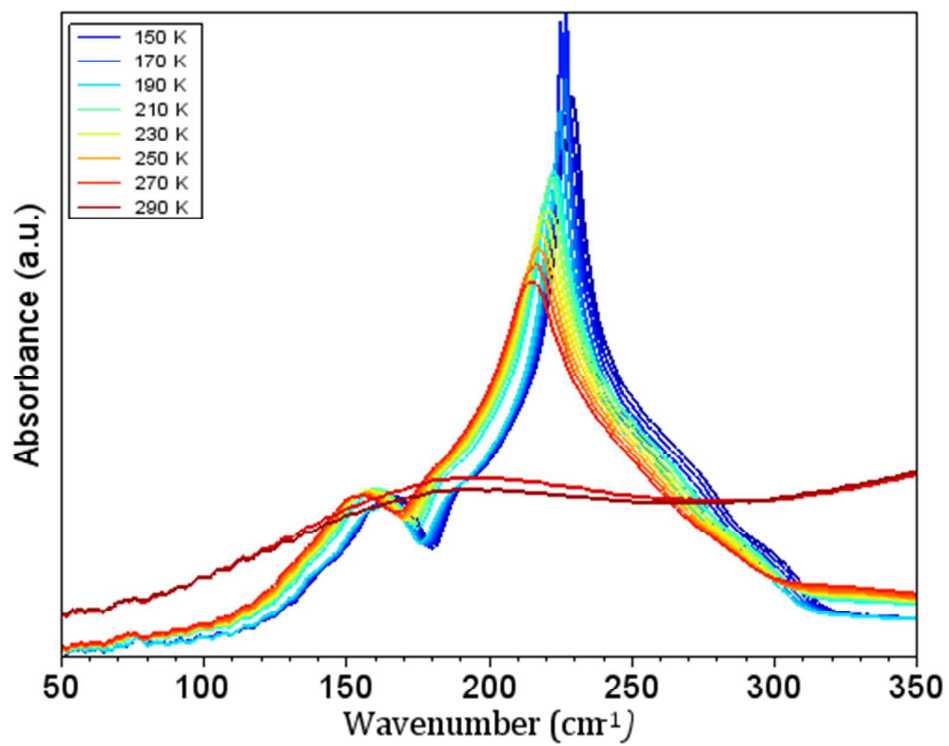
Figure 8.



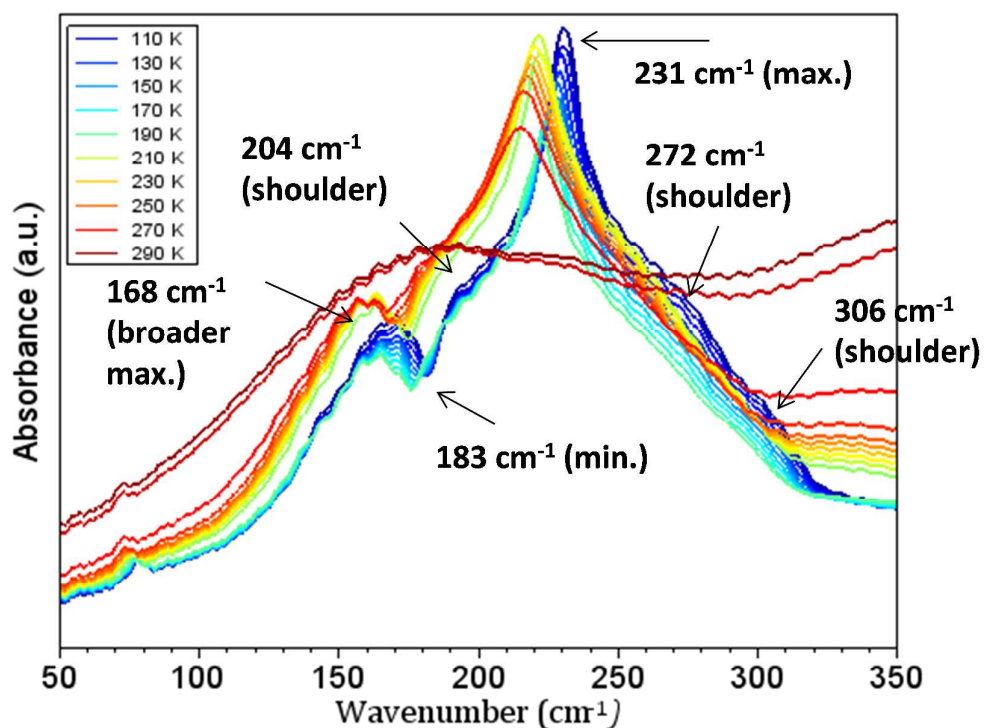
Far infrared spectra of ice and water. The temperature ranges from 100 K (blue) to 280 K (brown). Spectra are recorded by increasing the temperature in steps of 10 K. At 280 K, the spectrum of liquid water is recorded (brown). The main features of the band obtained at 100 K are indicated in the figure.

Figure 9.

(a)

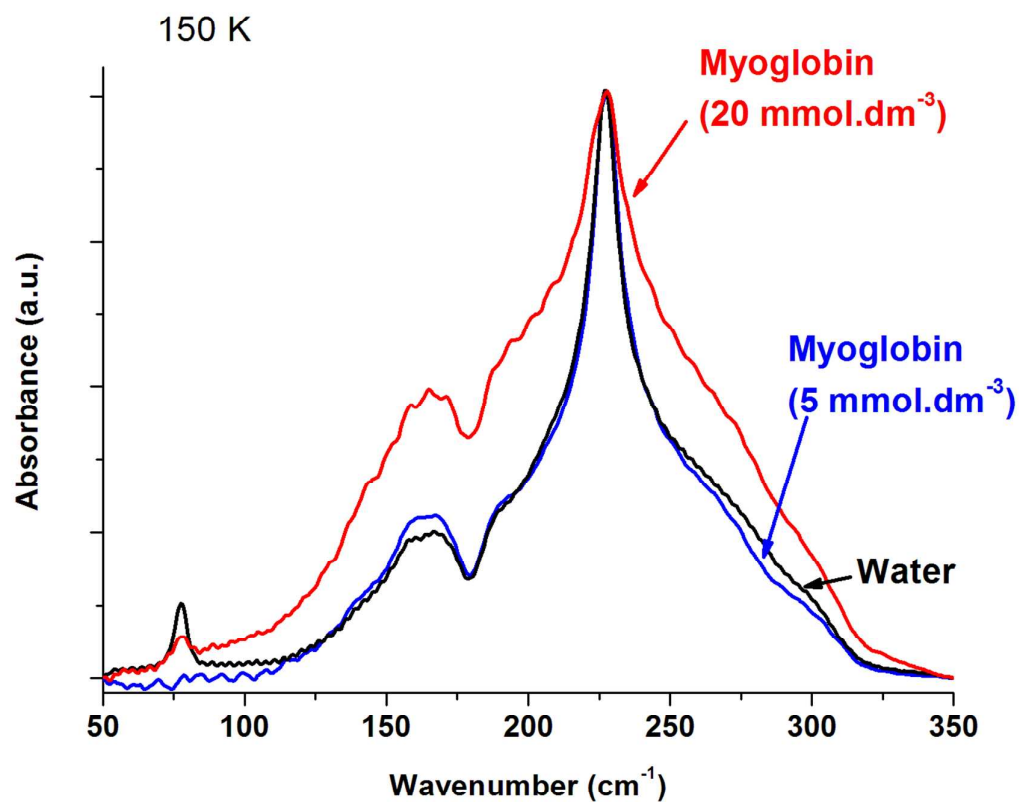


(b)



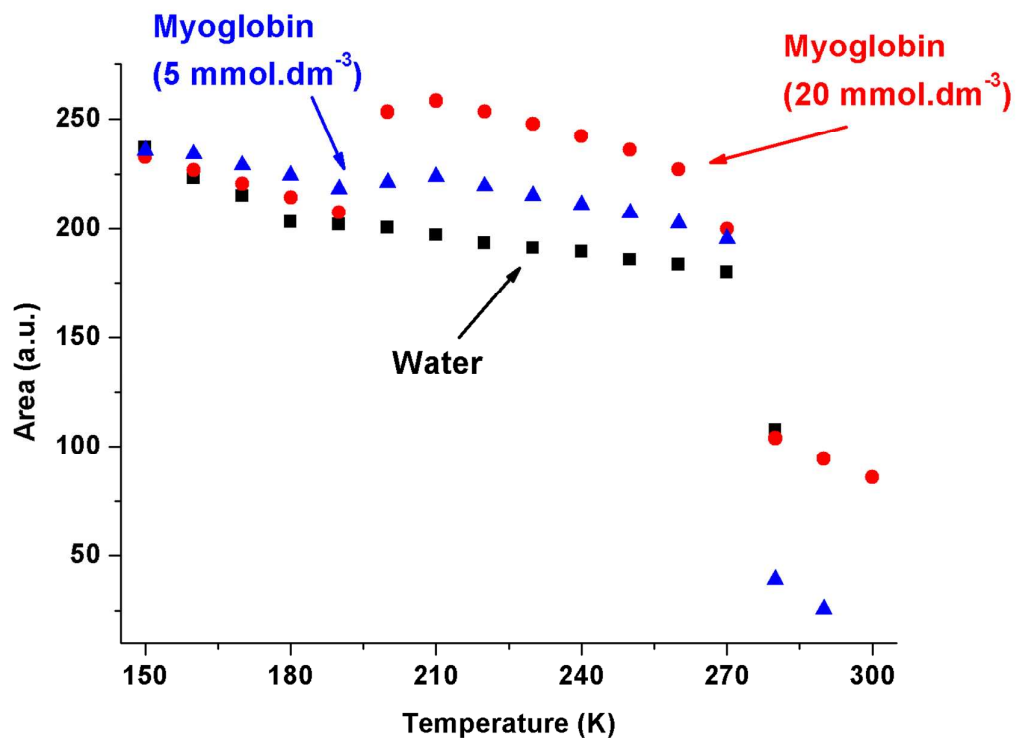
Far infrared spectra for a 5 mmol.dm<sup>-3</sup> myoglobin solution (9a) and a 20 mmol.dm<sup>-3</sup> myoglobin solution (9b). The temperature increases from 140 K (blue) to 290 K (brown) in steps of 10 K in Figure 9a; and from 100 K (blue) to 290 K (brown) in Figure 9b. The main features of the band obtained at 100 K are indicated in figure 9b for the 20 mmol.dm<sup>-3</sup> myoglobin sample.

Figure 10.



Comparison of the three far infrared spectra (water, in black; starting from a  $5 \text{ mmol} \cdot \text{dm}^{-3}$  myoglobin solution, in blue, and from a  $20 \text{ mmol} \cdot \text{dm}^{-3}$  myoglobin solution, in red) obtained at 150 K and normalized to the most intense band. The full width at half maximum of the band is equal to  $76 \text{ cm}^{-1}$  for the  $20 \text{ mmol} \cdot \text{dm}^{-3}$  myoglobin solution, whereas it is  $27 \text{ cm}^{-1}$  in the two other samples.

Figure 11.



Evolution of the area of the bands in the  $50\text{-}350\text{ cm}^{-1}$  spectral region after subtraction of the librational contributions as a function of the temperature for water (black squares), for the  $5\text{ mmol.dm}^{-3}$  myoglobin system (blue triangles) and for the  $20\text{ mmol.dm}^{-3}$  myoglobin sample (red circles). For the two latter systems, a clear jump in the band area is seen around 200 K. This jump does not exist in water for which the band area decreases regularly when the temperature increases. The band areas are normalized to the area recorded at 150 K.

## References

- 1 M. Ferrand, A. J. Dianoux, W. Petry and G. Zaccai, Thermal Motions and Function of Bacteriorhodopsin in Purple Membranes: Effects of Temperature and Hydration Studied By Neutron Scattering, *Proc. Natl. Acad. Sci. USA*, 1993, **90**, 9668.
- 2 P. W. Fenimore, H. Frauenfelder, B. H. McMahon and F. G. Parak, Slaving: Solvent Fluctuations Dominate Protein Dynamics and Functions, *Proc. Natl. Acad. Sci. USA*, 2002, **99**, 16047.
- 3 P. W. Fenimore, H. Frauenfelder, B. H. McMahon and R. D. Young, Bulk-Solvent and Hydration-Shell Fluctuations, Similar To Alpha- and Beta-Fluctuations in Glasses, Control Protein Motions and Functions, *Proc. Natl. Acad. Sci. USA*, 2004, **101**, 14408.
- 4 W. Doster, S. Cusack and W. Petry, Dynamical transition of Myoglobin Revealed by Inelastic Neutron Scattering, *Nature*, 1989, **337**, 754.
- 5 H. Frauenfelder, S. G. Sligar and P. G. Wolynes, The Energy Landscapes and Motions of Proteins, *Science*, 1991, **254**, 1598.
- 6 M. Tarek and D. J. Tobias, Role of Protein-Water Hydrogen Bond Dynamics in the Protein Dynamical Transition, *Phys. Rev. Lett.* , 2002, **88**, 138101.
- 7 D. Ringe and G. A. Petsko, The "Glass Transition" in Protein Dynamics: What It Is, Why It Occurs and How To Exploit It, *Biophys. Chem.* , 2003, **105**, 667.
- 8 D. Russo, J. R. D. Copley, J. Ollivier and J. Teixeira, On the Behaviour of Water Hydrogen Bonds at Biomolecular Sites: Dependences on Temperature and on Network Dimensionality, *J. Molecular Struct.* , 2010, **972**, 81.
- 9 A. P. Minton and J. Wilf, Effect of Macromolecular Crowding upon the Structure and Function of an Enzyme: Glyceraldehyde-3-phosphate Dehydrogenase, *Biochemistry*, 1981, **20**, 4821.
- 10 U. Heugen, G. Schwaab, E. Bründermann, M. Heyden, X. Yu, D. M. Leitner and M. Havenith, Solute-Induced Retardation of Water Dynamics Probed Directly by Terahertz Spectroscopy, *Proc. Natl. Acad. Sci. USA*, 2006, **103**, 12301.
- 11 E. Antonini and M. Brunori, North-Holland Publishing Company, Amsterdam-London, **1971**, p. 436.
- 12 S. J. Edelstein and H. K. Schachman, The Simultaneous Determination of Partial Specific Volumes and Molecular Weights with Microgram Quantities, *J. Biol. Chem.* , 1967, **242**, 306.
- 13 J.-B. Brubach, L. Manceron, M. Rouzies, O. Pirali, D. Balcon, F. K. Tchana, V. Boudon, M. Tudorie, T. Huet, A. Cuisset and P. Roy, in *WIRMS 2009: 5<sup>TH</sup> International Workshop on Infrared Microscopy and Spectroscopy with Accelerator Based Sources, Vol. 1214* (Eds.: A. PredoiCross, B. E. Billingham), Banff, Canada, **2010**, pp. 81.
- 14 P. Roy, M. Rouzies, Z. M. Qi and O. Chubar, The AILES Infrared Beamline on the Third Generation Synchrotron Radiation Facility SOLEIL, *Infrared Phys. Technol.* , 2006, **49**, 139.
- 15 S. Le Caër, D. J. Palmer, M. Lima, J. P. Renault, G. Vigneron, R. Righini and S. Pommeret, Time-Resolved Studies of Water Dynamics and Proton Transfer at the Alumina-Air Interface, *J. Am. Chem. Soc.*, 2007, **129**, 11720.
- 16 S. Le Caër, M. Lima, D. Gosset, D. Simeone, F. Bergaya, S. Pommeret, J. P. Renault and R. Righini, Dynamics of Water Confined in Clay Minerals, *J. Phys. Chem. C*, 2012, **116**, 12916.
- 17 J.-B. Brubach, A. Mermet, A. Filabozzi, A. Gerschel and P. Roy, Signatures of the Hydrogen Bonding in the Infrared Bands of Water, *J. Chem. Phys.*, 2005, **122**, 184509.
- 18 S. Le Caër, S. Pin, S. Esnouf, Q. Raffy, J. P. Renault, J.-B. Brubach, G. Creff and P. Roy, A Trapped Water Network in Nanoporous Material: the Role of Interfaces, *Phys. Chem. Chem. Phys.*, 2011, **13**, 17658.
- 19 E. Whalley and J. E. Bertie, The Far Infrared Spectrum and Long-Range Forces in Ice, *J. Colloid Interface Sci.* , 1967, **25**, 161.



- 20 C. Medcraft, D. McNaughton, C. D. Thompson, D. R. T. Appadoo, S. Bauerecker and E. G. Robertson, Water Ice Nanoparticles: Size and Temperature Effects on the Mid-Infrared Spectrum, *Phys. Chem. Chem. Phys.*, 2013, **15**, 3630.
- 21 A. Barth, Infrared Spectroscopy of Proteins, *Biochimica Biophysica Acta*, 2007, **1767**, 1073.
- 22 B. Jana, S. Pal and B. Bagchi, Hydration Dynamics of Protein Molecules in Aqueous Solution: Unity Among Diversity, *J. Chem. Sci.*, 2012, **124**, 317.
- 23 R. S. Knox and H. van Amerongen, Refractive Index Dependence of the Förster Resonance Excitation Transfer Rate, *J. Phys. Chem. B*, 2002, **106**, 5289.
- 24 R. Barer and S. Traczyk, Refractive Index of Concentrated Protein Solutions, *Nature*, 1954, **173**, 821.
- 25 W. M. Irvine and J. B. Pollack, Infrared Optical Properties of Water and Ice Spheres, *Icarus*, 1968, **8**, 324.
- 26 W. Chen, M. Sharma, R. Resta, G. Galli and R. Car, Role of Dipolar Correlations in the Infrared Spectra of Water and Ice, *Phys. Rev. B*, 2008, **77**, 245114.
- 27 M. Heyden, J. Sun, H. Forbert, G. Mathias, M. Havenith and D. Marx, Understanding the Origins of Dipolar Couplings and Correlated Motion in the Vibrational Spectrum of Water, *J. Phys. Chem. Lett.*, 2012, **3**, 2135.
- 28 R. Harada, Y. Sugita and M. Feig, Protein Crowding Affects Hydration Structure and Dynamics, *J. Am. Chem. Soc.*, 2012, **134**, 4842.
- 29 T. Miyazawa, T. Shimanouchi and S. Mizushima, Normal Vibrations of N-Methylacetamide, *J. Chem. Phys.*, 1958, **29**, 611.
- 30 P. Hamm, M. Lim and R. M. Hochstrasser, Structure of the Amide I Band of Peptides Measured by Femtosecond Nonlinear-Infrared Spectroscopy, *J. Phys. Chem. B*, 1998, **102**, 6123.
- 31 K. A. Peterson, C. W. Rella, J. R. Engholm and H. A. Schwettman, Ultrafast Vibrational Dynamic of the Myoglobin Amide I Band, *J. Phys. Chem. B*, 1999, **103**, 557.
- 32 M. F. Kropman, H.-K. Nienhuys, S. Woutersen and H. J. Bakker, Vibrational Relaxation and Hydrogen-Bond Dynamics of HDO:H<sub>2</sub>O, *J. Phys. Chem. A*, 2001, **105**, 4622.
- 33 S. Woutersen and H. J. Bakker, Resonant Intermolecular Transfer of Vibrational Energy in Liquid Water, *Nature*, 1999, **402**, 507.
- 34 K. J. Gaffney, I. R. Piletic and M. D. Fayer, Orientational Relaxation and Vibrational Excitation Transfer in Methanol-Carbon Tetrachloride Solutions, *J. Chem. Phys.*, 2003, **118**, 2270.
- 35 H. J. Bakker and H.-K. Nienhuys, Delocalization of Protons in Liquid Water, *Science*, 2002, **297**, 587.
- 36 Y. L. A. Rezus and H. J. Bakker, On the Orientational Relaxation of HDO in Liquid Water, *J. Chem. Phys.*, 2005, **123**, 114502.
- 37 S. Perticaroli, L. Comez, M. Paolantoni, P. Sassi, L. Lupi, D. Fioretto, A. Paciaroni and A. Morresi, Broadband Depolarized Light Scattering Study of Diluted Protein Aqueous Solutions, *J. Phys. Chem. B*, 2010, **114**, 8262.
- 38 P. J. Steinbach and B. R. Brooks, Protein Hydration Elucidated by Molecular Dynamics Simulation, *Proc. Natl. Acad. Sci. USA*, 1993, **90**, 9135.
- 39 J. E. Bertie and E. Whalley, Optical Spectra of Orientationally Disordered Crystals. II. Infrared Spectrum of Ice Ih and Ice Ic from 360 to 50 cm<sup>-1</sup>, *J. Chem. Phys.*, 1967, **46**, 1271.
- 40 X. He, O. Sode, S. S. Xantheas and S. Hirata, Second-Order Many-Body Perturbation Study of Ice Ih, *J. Chem. Phys.*, 2012, **137**, 204505.
- 41 J. S. Tse and D. D. Klug, Comments on "Further Evidence for the Existence of Two Kinds of H-Bonds in Ice Ih", *Phys. Lett. A*, 1995, **198**, 464.
- 42 M. Heyden, J. Sun, S. Funkner, G. Mathias, H. Forbert, M. Havenith and D. Marx, Dissecting the THz spectrum of liquid water from first principles via correlations in time and space, *Proc. Natl. Acad. Sci. USA*, 2010, **107**, 12068.

- 43 T. A. Lima, E. T. Sato, E. T. Martins, P. Homem-de-Mello, A. F. Lago, M. D. Coutinho-Neto, F. F. Ferreira, C. Giles, M. O. C. Pires and H. Martinho, Anharmonic Transitions in Nearly Dry L-Cysteine I, *J. Phys.: Condens. Matter*, 2012, **24**, 195104.
- 44 C. Zhang, E. Tarhan, A. K. Ramdas, A. M. Weiner and S. M. Durbin, Broadened Far-Infrared Absorption Spectra for Hydrated and Dehydrated Myoglobin, *J. Phys. Chem. B*, 2004, **108**, 10077.
- 45 R. L. Hudson and M. H. Moore, A Far-IR Study of Irradiated Amorphous Ice: An Unreported Oscillation between Amorphous and Crystalline Phases, *J. Phys. Chem.*, 1992, **96**, 6500.
- 46 J. Sadlej, An Attempt to Evaluate the Vibrational Intensity Changes due to Long-Range Interactions, *Adv. Molecul. Relax. Interact. Processes*, 1980, **16**, 149.
- 47 W. Doster, The Protein-Solvent Glass Transition, *Biochimica Biophysica Acta*, 2010, **1804**, 3.
- 48 A. L. Tournier, J. Xu and J. C. Smith, Translational Hydration Water Dynamics Drives the Protein Glass Transition, *Biophys. J.*, 2003, **85**, 1871.
- 49 K. Wood, A. Frölich, A. Paciaroni, M. Moulin, M. Härtlein, G. Zaccai, D. J. Tobias and M. Weik, Coincidence of Dynamical Transitions in a Soluble Protein and Its Hydration Water: Direct Measurements by Neutron Scattering and MD Simulations, *J. Am. Chem. Soc. Comm.*, 2008, **130**, 4586.
- 50 S. Devineau, J. M. Zanotti, C. Loupiac, L. Zargarian, F. Neiers and S. R. Pin, J.P., Myoglobin on Silica: A Case Study of the Impact of Adsorption on Protein Structure and Dynamics, *Langmuir*, 2013, **29**, 13465.
- 51 J. Liang, H. Edelsbrunner, P. Fu, P. V. Sudhakar and S. Subramaniam, Analytical Shape Computation of Macromolecules: I. Molecular Area and Volume Through Alpha Shape, *Proteins*, 1998, **33**, 1.
- 52 J. A. Rupley, E. Gratton and G. Careri, Water and Globular Proteins, *Trends Biochem. Sci.*, 1983, **8**, 18.
- 53 D. P. Goldenberg and B. Argyle, Self Crowding of Globular Proteins Studied by Small-Angle X-Ray Scattering, *Biophys. J.*, 2014, **106**, 895.
- 54 S. Torquato and M. Avellaneda, Diffusion and Reaction in Heterogeneous Media: Pore Size Distribution, Relaxation Times and Mean Survival Time, *J. Chem. Phys.*, 1991, **95**, 6477.
- 55 J.-B. Brubach, A. Mermet, A. Filabozzi, A. Gerschel, D. Lairez, M. P. Krafft and P. Roy, Dependence of water dynamics upon confinement size, *J. Phys. Chem. B*, 2001, **105**, 430.
- 56 A. Patra, T. Q. Luong, R. K. Mitra and M. Havenith, The Influence of Charge on the Structure and Dynamics of Water Encapsulated in Reverse Micelles, *Phys. Chem. Chem. Phys.*, 2014, **16**, 12875.
- 57 R. Musat, J. P. Renault, M. Candelaresi, D. J. Palmer, S. Le Caër, R. Righini and S. Pommeret, Finite Size Effects on Hydrogen Bonds in Confined Water, *Angew. Chem. Int. Ed. Engl.*, 2008, **47**, 8033.
- 58 S. E. Harding, Viscosity Parameters for Myoglobin, *IRCS Medical Science: Biochemistry; Cell and Membrane Biology; Hematology; Physiology*, 1980, **8**, 610.
- 59 A. B. Goins, H. Sanabria and M. N. Waxham, Macromolecular Crowding and Size Effects on Probe Microviscosity, *Biophys. J.*, 2008, **95**, 5362.
- 60 J. Szymanski, A. Patkowski, A. Wilk, P. Garstecki and R. Holyst, Diffusion and Viscosity in a Crowded Environment: from Nano- to Macroscale, *J. Phys. Chem. B*, 2006, **110**, 25593.
- 61 D. E. Moilanen, E. E. Fenn, Y.-S. Lin, J. L. Skinner, B. Bagchi and M. D. Fayer, Water inertial reorientation: hydrogen bond strength and the angular potential, *Proc. Natl. Acad. Sci. USA*, 2008, **105**, 5295.
- 62 M. Heyden and D. J. Tobias, Spatial Dependence of Protein-Water Collective Hydrogen-Bond Dynamics, *Phys. Rev. Lett.*, 2013, **111**, 218101.
- 63 V. Conti Nibali, G. D'Angelo, A. Paciaroni, D. J. Tobias and M. Tarek, On the Coupling between the Collective Dynamics of Proteins and Their Hydration Water, *J. Phys. Chem. Lett.*, 2014, **5**, 1181.

- 64 A. Paciaroni, A. Orecchini, E. Cornicchi, M. Marconi, C. Petrillo, M. Haertlein, M. Moulin and F. Sacchetti, Coupled Thermal Fluctuations of Proteins and Protein Hydration Water on the Picosecond Timescale, *Philosophical Magazine*, 2008, **88**, 4071.
- 65 S. Khodadadi, J. H. Roh, A. Kisiuk, E. Mamontov, M. Tyagi, S. A. Woodson, R. M. Briber and A. P. Sokolov, Dynamics of Biological Macromolecules: Not a Simple Slaving by Hydration Water, *Biophys. J.*, 2010, **98**, 1321.